Molecular Biology of the Cell
Vol. 13, 3930–3942, November 2002

Phospholipase D2 Is Localized to the Rims of the Golgi Apparatus in Mammalian Cells

Zachary Freyberg,* Sylvain Bourgoin,† and Dennis Shields*‡§

*Departments of Developmental and Molecular Biology and ‡Anatomy and Structural Biology, Albert Einstein College of Medicine, Bronx, New York 10461; and †Centre de Recherche en Rhumatologie et Immunologie, Centre de Recherche du CHUL, Ste-Foy, Quebec, Canada G1V 4G2

Submitted April 22, 2002; Revised August 20, 2002; Accepted August 22, 2002
Monitoring Editor: Suzanne R. Pfeffer

Phospholipase D (PLD) hydrolyzes phosphatidylcholine to generate phosphatidic acid, a molecule known to have multiple physiological roles, including release of nascent secretory vesicles from the *trans*-Golgi network. In mammalian cells two forms of the enzyme, PLD1 and PLD2, have been described. We recently demonstrated that PLD1 is localized to the Golgi apparatus, nuclei, and to a lesser extent, plasma membrane. Due to its low abundance, the intracellular localization of PLD2 has been characterized only indirectly through overexpression of chimeric proteins. Using antibodies specific to PLD2, together with immunofluorescence microscopy, herein we demonstrate that a significant fraction of endogenous PLD2 localized to the perinuclear Golgi region and was also distributed throughout cells in dense cytoplasmic puncta; a fraction of which colocalized with caveolin-1 and the plasma membrane. On treatment with brefeldin A, PLD2 translocated into the nucleus in a manner similar to PLD1, suggesting a potential role in nuclear signaling. Most significantly, cryoimmunogold electron microscopy demonstrated that in pituitary GH_3 cells >90% of PLD2 present in the Golgi apparatus was localized to cisternal rims and peri-Golgi vesicles exclusively. The data are consistent with a model whereby PLD2 plays a role in Golgi vesicular transport.

INTRODUCTION

In the past five years, an increasing body of evidence has pointed to the crucial importance of phospholipids in mediating signal transduction and intracellular trafficking (De Camilli *et al.*, 1996; Cremona and De Camilli, 2001; Martin, 2001). Indeed, cells use an array of lipid modifying enzymes, many of which have multiple isoforms, that control the spatial and temporal localization of specific phospholipids. Lipid kinases such as phosphatidylinositol 4- and 5-kinases phosphorylate phosphoinositide phospholipids on the membranes to which they are recruited and localized in a stereospecific manner. The resulting product, phosphatidylinositol (4,5)-bisphosphate [PtdIns(4,5)P_2], both localizes and interacts with proteins to mediate intracellular vesicular transport and signal transduction. In contrast to phosphatidylinositol kinases, phospholipase D (PLD) catalyzes the hydrolysis of phospholipids, primarily phosphatidylcholine, to generate phosphatidic acid (PA). PLD-generated PA has multiple functions within the cell, including promotion of PtdIns(4,5)P_2 synthesis through stimulation of phosphatidylinositol 4-phosphate 5-kinase activity (Jenkins *et al.*, 1994; Honda *et al.*, 1999; Siddhanta *et al.*, 2000). Additionally, PA signaling is implicated in a diverse range of processes such as exocytosis, endocytosis, intracellular vesicular transport, and maintenance of the Golgi structure, further underscoring the importance of PLD and PA in cellular function (Siddhanta *et al.*, 2000; Cremona and De Camilli, 2001; Sweeney *et al.*, 2002).

Phospholipase D is present in many species from yeast to humans (Liscovitch *et al.*, 2000). In mammals, PLD exists as two major isoforms, PLD1 and PLD2. PLD1, a 1074-amino acid protein, is exquisitely sensitive to stimulation by the small GTP-binding protein ADP-ribosylation factor 1 (ARF1). It has been demonstrated to play a role in release of nascent secretory vesicles from the *trans*-Golgi network in an ARF1-dependent manner (Ktistakis *et al.*, 1996; Chen *et al.*, 1997). Similarly, PLD1 may also be important in regulation of exocytic neurotransmitter release at the neuronal plasma membrane (Humeau *et al.*, 2001). Recent work has also demonstrated that PLD1 activity is necessary in the formation of actin stress fibers (Kam and Exton, 2001). In addition to ARF1, PLD1 activity is stimulated by interactions with other small GTP-binding proteins: RhoA, Rac-1, and Cdc42 (Hammond *et al.*, 1997). Regulation of PLD1 activity by these molecules as well as through phosphorylation by protein

Article published online ahead of print. Mol. Biol. Cell 10.1091/mbc.02–04–0059. Article and publication date are at www.molbiolcell.org/cgi/doi/10.1091/mbc.02–04–0059.

§ Corresponding author. E-mail address: shields@aecom.yu.edu.

kinase Cα (Hammond *et al.*, 1997) points to PLD1 function in membrane dynamics and cytoskeletal remodeling. PLD1 has a somewhat heterogeneous intracellular distribution and overexpression experiments have localized it to the plasma membrane, endoplasmic reticulum (ER), Golgi apparatus, secretory granules, nucleus, and lysosomes (Colley *et al.*, 1997; Brown *et al.*, 1998; Kim *et al.*, 1999; Toda *et al.*, 1999; Baldassare *et al.*, 2001). However, consistent with a role in protein transport through the Golgi apparatus and vesicle release from the *trans*-Golgi network (Ktistakis *et al.*, 1996; Chen *et al.*, 1997), recent data from our laboratory demonstrated that ~30% of total endogenous cellular PLD1 is localized to Golgi cisternae (Freyberg *et al.*, 2001).

PLD2, a 933-amino acid protein, shares ~50% sequence identity with PLD1, including the catalytic domains; the enzymes vary primarily at their amino and carboxy termini. PLD1 and PLD2 also differ in their sensitivities to ARF1 and RhoA, whereas the catalytic activity of PLD1 is stimulated >13-fold by the GTP-bound form of ARF1, PLD2 exhibits only a 1.5-fold effect (Brown *et al.*, 1993; Colley *et al.*, 1997; Lopez *et al.*, 1998; Sung *et al.*, 1999). Similarly, RhoA has been demonstrated to stimulate PLD1 while having no effect on PLD2 activity (Sung *et al.*, 1999). However, recent work has described a powerful synergistic activation of PLD2 by ARF and other effectors such as G(M2) activator, a heat-stable activator of ganglioside metabolism, suggesting an interaction of multiple factors in the regulation of this enzyme (Sarkar *et al.*, 2001). Additionally, PLD2 activity may be regulated through interactions with receptor tyrosine kinases; for example, epidermal growth factor receptor (EGF-R) has been demonstrated to both associate with and stimulate PLD2 activity (Slaaby *et al.*, 1998). This association at the cell surface has also been implicated in regulating endocytosis of EGF-R (Shen *et al.*, 2001). Furthermore, overexpression of both PLD2 and EGF-R results in cellular transformation, suggesting a role for PLD2 in the complex control of mitogenic signaling (Joseph *et al.*, 2001).

Given the differences in the functional associations between PLD1 and PLD2, their subcellular distributions also vary. In contrast to PLD1, previous studies in which PLD2 was overexpressed identified the plasma membrane as the major site of its localization (Colley *et al.*, 1997). Consistent with these results, other studies demonstrated interactions between heterologously expressed PLD2, EGF-R, and ARF6, a plasma membrane-localized ARF isoform, particularly at sites of plasma membrane ruffling (Honda *et al.*, 1999). Subcellular fractionation also revealed that PLD2, unlike PLD1, cofractionated with caveolin-1 in low-density membrane fractions derived from human keratinocyte cells, further pointing to a role for PLD2 in regulation of membrane dynamics (Czarny *et al.*, 1999, 2000). However, given discrepancies in the distribution of endogenous vs. overexpressed PLD1, we wished to determine the intracellular localization of endogenous PLD2. In this study, we demonstrate that although some PLD2 is localized to the plasma membrane, ~20% of the enzyme was localized to the Golgi apparatus. Most significantly, in contrast to PLD1, which is distributed throughout the Golgi apparatus, PLD2 was present almost exclusively on the rims of the Golgi cisternae.

MATERIALS AND METHODS

Antibodies

A rabbit antibody to PLD2, termed PLD2-27, was raised against a mixture of two peptides: ^{823}GANTRPDLDLRDPICDD^{839} (human) and ^{483}QTPTPGSDPAATPDLSH^{499} (rat) (Houle and Bourgoin, 1999). An independently generated rabbit polyclonal antibody, designated PLD2-42, directed against a peptide in the NH_2 terminus of human PLD2 (^{13}DELDSSQLQMESDEVDTKE^{33}) was used in some experiments. A rabbit polyclonal antibody to PLD1 designated P1-P4 (Marcil *et al.*, 1997), described in Freyberg *et al.* (2001), was also used. Mouse monoclonal antibody (mAb) to mannosidase II (53FC3) was provided by Dr. Brian Burke (University of Calgary, Calgary, Alberta, Canada); rabbit anti-rat lgp120 was a kind gift from Dr. Ira Mellman (Yale University Medical School, New Haven, CT). Mouse monoclonal antibodies to GM130 and caveolin-1 were purchased from BD Transduction Laboratories (San Diego, CA); mouse monoclonal antibodies to BiP were purchased from Stressgen (San Diego, CA). Purified monoclonal anti-rat transferrin receptor antibodies were purchased from Cedarlane Laboratories (Hornby, Ontario, Canada). Alexa green-conjugated goat anti-mouse and Alexa red-conjugated goat anti-rabbit secondary antibodies were purchased from Molecular Probes (Eugene, OR).

Immunofluorescence Microscopy

Rat GH_3 and normal rat kidney (NRK) cells were grown on poly-L-lysine–coated glass coverslips as described previously (Austin and Shields, 1996; Lowe *et al.*, 2000). Cells were either untreated or pretreated with 5 μg/ml brefeldin A (BFA) for 5, 10, 20, or 40 min, and 10 μM nocodazole for 4 h at 37°C, and fixed in 3% paraformaldehyde. Samples were incubated for 1 h at room temperature with primary antibodies diluted in solution I (0.5% bovine serum albumin, 0.2% saponin, 1% fetal calf serum in phosphate-buffered saline) before use. Some samples were treated with primary antibodies preincubated in solution I for 1 h with rotation at room temperature with peptides against which the PLD antibodies were raised. The samples were then treated with appropriate secondary antibodies also diluted in solution I. After extensive washing, the coverslips were mounted onto slides and examined using an Olympus (Melville, NY) IX 70 microscope with 60× numerical aperture 1.4 planapo optics by using a Photometrics (Tucson, AZ) Censys cooled charge-coupled device camera. Z series images were obtained through the depth of cells by using a step size range of 0.1–0.4 μm and projected using the maximum pixel method. Deconvolution was performed with Vaytek (Fairfield, IA) PowerHazeBuster running on a Macintosh G3 and maximum pixel projections were rendered with I.P. Lab Spectrum (Scanalytics, Fairfax, VA). Images were processed using Adobe Photoshop software (Abode Systems, Mountain View, CA) at identical settings. Controls were imaged so as to rule out background fluorescence or bleed-through between Alexa green and red channels.

Quantitative Cryoimmunogold Electron Microscopy

GH_3 cells were fixed in 4% paraformaldehyde, 0.1% glutaraldehyde, 0.25 M HEPES, pH 7.4, and embedded in 10% gelatin. The cells were cryoprotected by infiltration with 2.3 M sucrose in phosphate-buffered saline. After liquid nitrogen freezing, 90-nm sections were cut using a Leica (Nussloch, Germany) UCT cryoultramicrotome. Sections were placed on grids and immunolabeled with peptide affinity-purified antibodies against PLD2 followed by goat anti-rabbit IgG conjugated to 10-nm gold particles (Aurion, Wageningen, The Netherlands). Samples were then treated with 2% uranyl acetate, pH 7.0, and embedded in 0.75% methylcellulose. The grids were examined using a 1200 EX transmission electron microscope (JEOL, Peabody, MA). Quantitation of the subcellular distribution of PLD2 was performed by counting the total number of PLD2 immunore-

active gold particles in 58 cells. The amount of gold particles found in the cytoplasm and membrane-bound organelles was expressed as a percentage of the total within cells. The fraction of gold particles on caveolae was quantified independently of the plasma membrane fraction. Golgi rims were defined as the final 50 nm of the lateral ends of individual cisternae. The number of gold particles at cisternal rims was expressed as the percentage of the total number of gold particles distributed throughout the Golgi apparatus.

Stereological Analysis

GH_3 cells were prepared for transmission electron microscopy as described previously (Siddhanta *et al.*, 2000), and random sections were used in all stereological analyses. The cells were randomly photographed at low (level I; 5,400×) and intermediate (level II; 13,500×) magnifications, whereas Golgi stacks were photographed at high (level III; 30,000×) magnification (Griffiths *et al.*, 1989). All measurements were made from printed 8- × 10-inch images of each cell and expressed as the mean ± SEM.

Estimation of Volume Density. The mean cellular volume density was estimated using random micrographs of GH_3 cells taken at low and intermediate magnifications; 54 individual cells were counted. The average volume densities of the cytoplasm and organelles were measured by overlaying square lattice grids on the micrographs. The volume density of an organelle [$V_{(org)}$] was determined by counting the number of intersecting points on the grid in both vertical and horizontal directions and expressing a ratio of points on the organelle [$P_{(org)}$] to the total number of points over the reference space, the cell [$P_{(cell)}$] (Griffiths, 1993). The individual organellar volume densities were expressed as a percentage. The cytoplasmic volume density was derived by subtracting the sum of all organellar volume densities from the total cellular volume density.

Estimation of Membrane Surface Area. The relative ratio of plasma membrane-to-Golgi surface area was determined by overlaying a grid of parallel lines randomly on an assortment of 8- × 10-inch micrographs of low and intermediate magnification; 55 individual cells were used in the determination. Intersections of the parallel lines with either the plasma or Golgi membranes were counted. The surface density, S_v, was estimated using the following formula:

$$S_{v(org)} = \frac{\sum_{i=1}^{n} I_i}{\sum_{i=1}^{n} P_i}$$

where I is the number of intersections of the respective membrane with the grid, and P is the total number of counts on the cell. The ratio of plasma membrane to Golgi surface areas was determined by dividing individual surface density values for the plasma membrane, S_{pm}, by that of the Golgi apparatus, S_{ga}.

Determination of PLD2 Enrichment in the Golgi Apparatus. To determine the enrichment of PLD2-immunoreactive gold particles in the Golgi apparatus relative to other organelles, first the ratio of the absolute fraction of gold particles in a specific organelle, $G_{(org)}$, (expressed as a percentage; Table 1) to the organelle's volume density, $S_{v(org)}$, was calculated as follows:

$$C_{g,v(org)} = \frac{G_{(org)}}{S_{v(org)}}$$

where $C_{g,v}$ is a coefficient. The enrichment of PLD2 per volume density for the Golgi apparatus relative to a given organelle was then calculated by dividing the $C_{g,v}$ for the Golgi apparatus by the $C_{g,v}$ for each organelle (Table 2A).

This method was also applied to determine PLD2 enrichment in the Golgi apparatus relative to the plasma membrane, where surface density rather than volume density was used (Table 2B). In this case, $C_{g,s}$ rather than $C_{g,v}$ was used as the coefficient.

Quantitation of Golgi Rims. Using high-magnification micrographs of Golgi cisternae, the fraction of cisternae constituting rims was calculated by dividing the length of the terminal 50 nm of cisternae by the absolute length of the cisternae; 178 individual cisternae were counted. The relative enrichment of PLD2 immunoreactive gold particles in rims was determined by dividing the ratio of percentage of PLD2 gold in rims to percentage of rim fraction by the ratio of percentage of PLD2 gold in the remainder of the cisternae to percentage of fraction of remainder of cisternae.

Table 1. Intracellular localization of PLD2

A

Organelle	Total gold particles (%)
Endoplasmic reticulum	7.6 ± 2.2
Golgi apparatus	19.2 ± 0.2
Plasma membrane	15.7 ± 5.0
Mitochondria	6.6 ± 0.6
Nucleus	20.5 ± 9.0
Cytoplasm	21.9 ± 1.5
Caveolae	8.5 ± 2.7

B

Distribution of PLD2 within organelles	Total gold particles (%)
Golgi apparatus	
Cisternae	5.9 ± 4.1
Rims	94.1
Plasma membrane	
Membrane	73.8 ± 6.7
Filopodia	26.2

C

Golgi rim fraction (%)	PLD2 Golgi rim enrichment (fold)	PLD1 Golgi rim enrichment (fold)
16.6 ± 0.3	80.2	1.7

A: The intracellular localization of PLD2 immunoreactive gold particles was quantitated from electron micrographs of GH_3 cells (N = 58; MATERIALS AND METHODS). The fraction of gold particles on caveolae was quantified independently of the plasma membrane fraction.

B: The numbers of gold particles distributed on Golgi cisternal rims and plasma membrane filopodia were expressed as a percentage of the total immunoreactive gold localized on the respective organelle.

C: The fraction of Golgi rims relative to cisternae was quantitated from electron micrographs of GH_3 cells (N = 178) and the relative enrichment of immunoreactive PLD2 gold particles in rims was determined (MATERIALS AND METHODS).

Table 2. Relative enrichment of PLD2

A Organelle	Organelle volume (V_{org}) (%)	$C_{g,v(org)}$	Relative PLD2 Golgi enrichment (fold) $C_{g,v(Golgi)}/C_{g,v(org)}$	Relative PLD1 Golgi enrichment (fold) $C_{g,v(Golgi)}/C_{g,v(org)}$
Nucleus	42.6% ± 1.4%	0.48	25.0	23.0
Cytoplasm	37.6% ± 1.5%	0.58	20.7	40.6
Mitochondria	10.9% ± 0.5%	0.61	19.7	11.1
ER	7.3% ± 0.4%	1.04	11.5	25.7
Golgi	1.6% ± 0.1%	12.00	1.0	1.0

B Organelle	Surface density ratio ($S_{v(org)}$)	$C_{g,s(org)}$	Relative PLD2 Golgi enrichment (fold) $C_{g,s(Golgi)}/C_{g,s(PM)}$	Relative PLD1 Golgi enrichment (fold) $C_{g,s(Golgi)}/C_{g,s(PM)}$
Plasma membrane	2.4 ± 0.1	0.22	2.9	4.5
Golgi apparatus	1.0	0.65	1.0	1.0

A: The volume percentages of organelles was quantitated from electron micrographs of GH_3 cells (N = 54; MATERIALS AND METHODS). The percentage of gold particles distributed on the organelles (Table I) was divided by the respective volume percentage (V_{org}) and expressed as $C_{g,v}$, the gold to volume ratio. This gives a relative measure of PLD2-immunoreactive gold per organellar membrane volume. The PLD2 enrichment in the Golgi apparatus relative to other organelles is also determined (Methods). The percent distributions of PLD1 gold particles were described previously (Freyberg *et al.*, 2001) and used to calculate relative PLD1 enrichment.

B: The ratio of plasma membrane surface area to Golgi membrane surface area was quantitated from electron micrographs of GH_3 cells (N = 55; MATERIALS AND METHODS). Analogous to A, the percentages of gold particles distributed on the plasma membrane or Golgi apparatus (Table 1) were divided by the respective surface area percentages ($C_{g,s}$). PLD1 and -2 enrichment in the Golgi apparatus relative to the plasma membrane are expressed as the ratio of $C_{g,s(Golgi)}$ to $C_{g,s(PM)}$.

RESULTS

PLD2 Localizes to Golgi Apparatus

Previous work from our laboratory demonstrated that in several cell types endogenous PLD1 has a diffuse cytoplasmic distribution and is enriched in the perinuclear Golgi apparatus and nucleus (Freyberg *et al.*, 2001). These findings contrasted with other reports that localized overexpressed PLD1 to endosomes and lysosomes (Brown *et al.*, 1998). In light of discrepancies between the distributions of endogenous PLD1 vs. the overexpressed enzyme, we predicted a similar difference in PLD2 localization. We therefore examined the intracellular localization of endogenous PLD2 in rat NRK cells by using indirect immunofluorescence microscopy. Endogenous PLD2 displayed perinuclear enrichment (Figure 1D) similar to that observed in PLD1 staining (Figure 1A). Costaining of the cells for the *medial*-Golgi marker mannosidase II revealed a high degree of overlap with both PLD1 and PLD2, consistent with localization of these enzymes to the Golgi apparatus (Figure 1, C and F, respectively). Cells treated with the anti-PLD2 antibody alone exhibited an identical perinuclear staining pattern, excluding the possibility that the Golgi staining resulted from overlap of the fluorescence signals between the PLD2 and mannosidase II channels (our unpublished data). In contrast to the diffuse cytoplasmic staining of PLD1, PLD2 also displayed dense puncta distributed throughout the cell. Although some cells manifested a limited degree of plasma membrane staining (Figure 2), this endogenous distribution differed markedly from overexpressed PLD2 that is localized primarily at the plasma membrane (Colley *et al.*, 1997). These findings are in agreement with our recent observations with subcellular fractionation that showed that in rat liver, PLD2 was evident mainly in fractions corresponding to Golgi and light membrane fractions (Sweeney *et al.*, 2002). In rat GH_3 cells, PLD2 had perinuclear enrichment as well as staining in the dense puncta distributed throughout the cytoplasm as seen in NRK cells. However, unlike NRK cells, some GH_3 cells also exhibited nuclear staining (Figure 2G). This nuclear localization in GH_3 cells relative to NRK cells was also seen in the case of PLD1 (Freyberg *et al.*, 2001), suggesting that both PLD enzymes may play a more prominent role in the nuclei of some cell types compared with others.

To determine whether PLD2 was distributed throughout the Golgi apparatus or limited to the *medial* compartment, NRK cells were costained with antibodies to both PLD2 (PLD2-27) and GM130, a *cis*-Golgi marker (Figure 2, A–C). PLD2 displayed the same overlap with GM130 as observed with mannosidase II (Figure 1, D–F), indicating that the enzyme was localized to multiple cisternae of the Golgi apparatus. PLDs are present in very low levels in most cells (Ganley *et al.*, 2001) and to control for the specificity of the antibody staining, anti-PLD2 antibodies were preincubated with increasing concentrations of PLD2 peptides (see MATERIALS AND METHODS) before immunofluorescence microscopy. As little as 1 μg of PLD2 peptides was sufficient to eliminate all the staining of PLD2 in NRK cells (Figure 2, E and F). Similarly, 1 μg of PLD2 peptides abolished all PLD2 staining in GH_3 cells (Figure 2, H and I), indicating specificity of PLD2 staining by the antibody in both cell types. Although unlikely, it was possible that the Golgi localization of PLD2 was due to cross-reaction with PLD1 present in the Golgi apparatus. To exclude this possibility, PLD2 antiserum was preincubated with up to 15 μg of PLD1-specific P1-P4 peptides (see MATERIALS AND METHODS). The resulting staining pattern was indistinguishable from that of

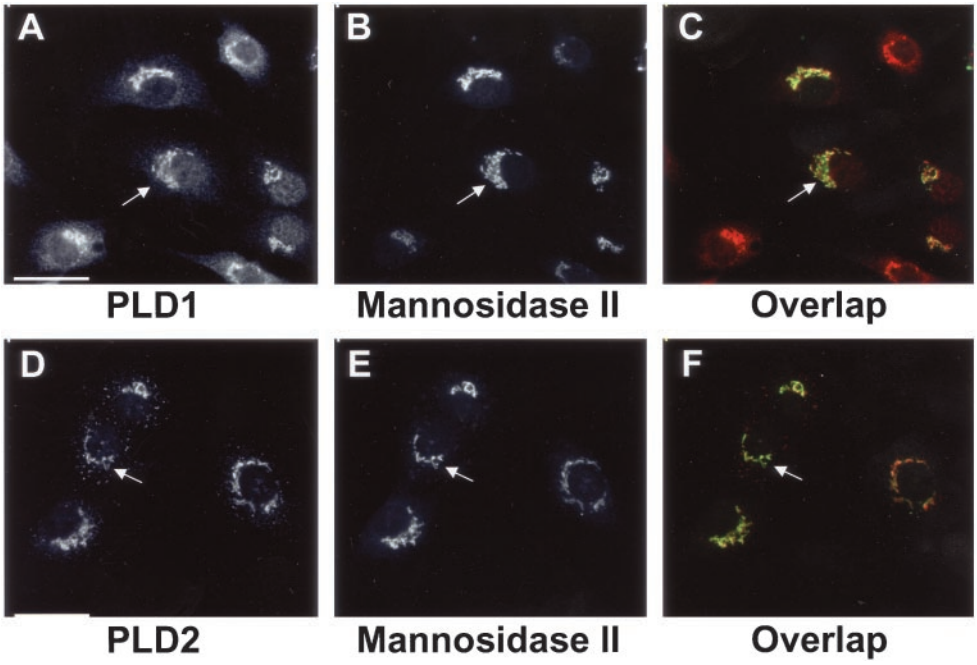

Figure 1. Comparison of PLD1 and PLD2 localization in rat NRK cells. NRK cells were prepared for double immunofluorescence microscopy (see MATERIALS AND METHODS) by using mAb 53FC3 to the *cis/medial*-Golgi marker mannosidase II (B and E) and either a rabbit antibody to PLD1 (A) or a rabbit antibody to PLD2, PLD2-27 (D). Mannosidase II was visualized using Alexa green-conjugated goat anti-mouse IgG, whereas PLD1 and PLD2 were localized with Alexa red-conjugated goat anti-rabbit IgG. Each sample is from the same field of cells. Images were merged to demonstrate overlap of PLD1 or PLD2 with mannosidase II (C and F); yellow regions demonstrate complete colocalization. Arrows indicate areas of PLD1 and PLD2 enrichment. All micrographs are projected Z-series images taken using a cooled charge-coupled device camera (see MATERIALS AND METHODS). Bars, 10 μm.

endogenous PLD2, ruling out cross-reaction with PLD1 and indicating the high degree of specificity of the antibody for endogenous PLD2 (Figure 2D). To eliminate the possibility of cross-reaction between the antibody and any other nonrelated antigens, a second polyclonal antibody raised against a peptide corresponding to a different region of PLD2 (see MATERIALS AND METHODS) was used. PLD2 staining with this antibody, designated PLD2-42, gave an identical perinuclear localization to that obtained using the PLD2-27 antibody (Figure 3, A and D). Furthermore, there was significant overlap between the mannosidase II and GM130 Golgi markers (Figure 3, C and F, respectively) and the PLD2-42 antibody staining, thus confirming the specificity of PLD2 localization.

The punctate staining of PLD2 led us to investigate the possibility that it localized to organelle(s) that share a similar appearance; consequently, we examined whether PLD2 colocalized with BiP, transferrin receptor, and lgp120, which are ER, early endosomal, and lysosomal markers, respectively. BiP had a diffuse reticular staining characteristic of the ER. However, the dense cytoplasmic PLD2-positive puncta did not overlap with the more diffuse, BiP distribution (Figure 4, A–C). This result was consistent with quantitative electron microscopy of the intracellular localization of PLD2, whereby the enzyme showed relatively little ER localization compared with its Golgi distribution (Table 1). In contrast, there was partial colocalization between transferrin receptor and PLD2; however, much of the overlap was in the Golgi region of the cells (Figure 4, D–F). Presumably, the colocalization at the Golgi apparatus was largely due to the dynamic recycling of transferrin receptor between the plasma membrane, endosomes, and Golgi apparatus. In spite of overlap at the Golgi apparatus and plasma membrane, the PLD2 puncta and those associated with transferrin receptor staining did not visibly colocalize to a large extent. Similarly, PLD2 staining did not exhibit a clear colocalization with lgp120 (Figure 4, G–I). As in the case of transferrin receptor, there was overlap between PLD2 and lgp120 in the perinuclear Golgi region, yet little if any in the cytoplasm because, like transferrin receptor, lgp120 shuttles between the Golgi apparatus and lysosomes. Some cells exhibited more PLD2 staining at the plasma membrane than others (Figure 4, D and J) underscoring its dynamic localization similar to that of transferrin receptor and lgp120. In contrast to these results, in NRK cells there was overlap between PLD2 and caveolin-1 (Figure 4, J–L). This finding was consistent with previous reports, indicating PLD2 is present on membrane fractions enriched in caveolin-1 (Czarny *et al.*, 1999, 2000). The staining of both PLD2 and caveolin-1 colocalized in the perinuclear Golgi region with a moderate degree of overlap throughout the cytoplasm. Close analysis revealed that many PLD2-positive puncta did not overlap completely with caveolae but were actually adjacent to these organelles. Taken together, these results indicate that PLD2 localizes to the perinuclear Golgi region with proteins that exit and/or recycle from the *trans*-Golgi compartment as well as to caveolae.

Brefeldin A and Nocodazole Treatments Alter PLD2 Localization

BFA and nocodazole disrupt the structure of the Golgi apparatus via very different mechanisms. In preventing ER-to-Golgi trafficking, BFA causes the Golgi apparatus to tubulate with redistribution of most Golgi proteins into the ER (Lippincott-Schwartz *et al.*, 1989; Ward *et al.*, 2001). Nocodazole treatment, in contrast, causes the Golgi apparatus to fragment into large vesicles at the cell periphery through disruption of the microtubule network. Given the differences that these two drugs exert on Golgi structure, we compared

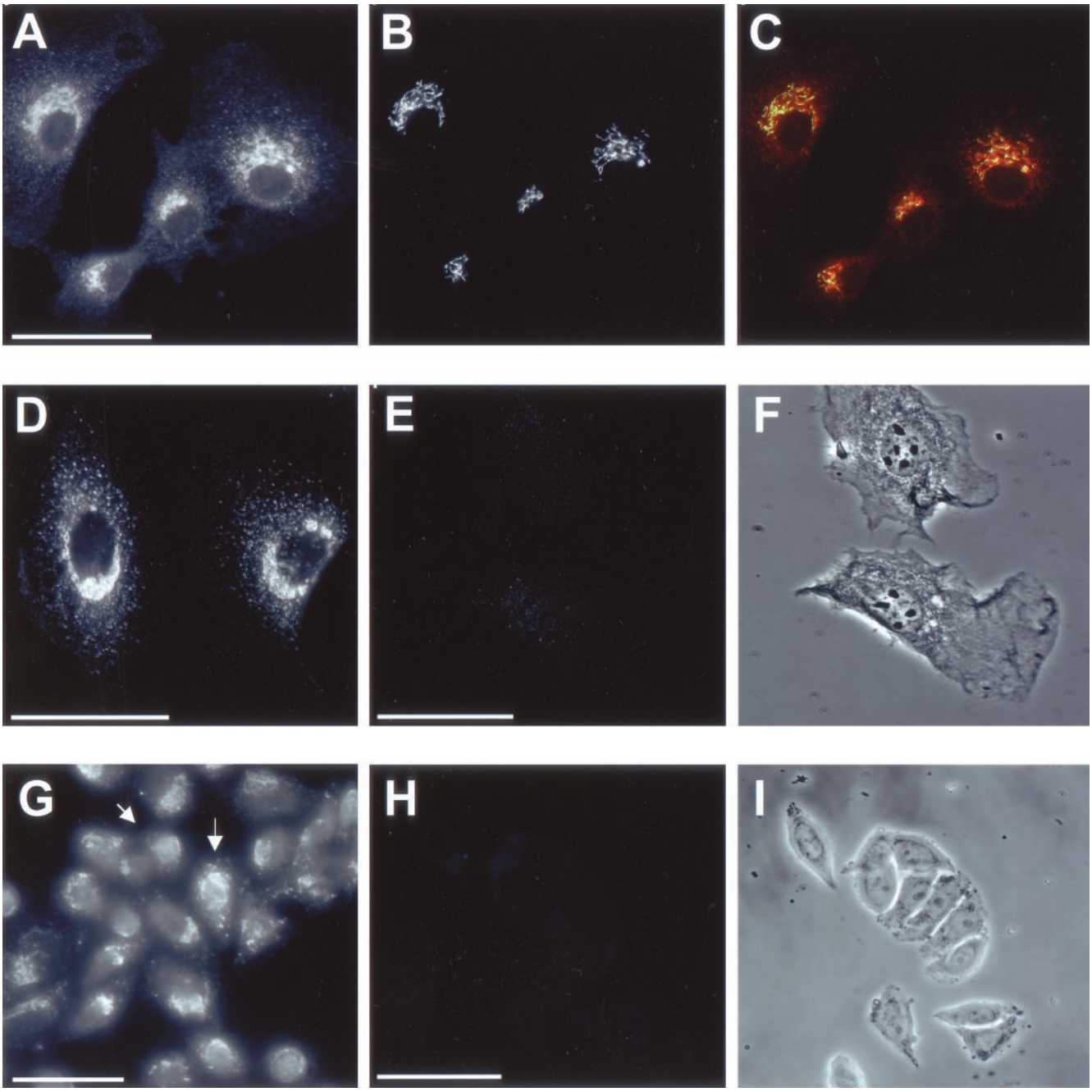

Figure 2. Immunolocalization of endogenous PLD2 in rat NRK and GH_3 cells. NRK cells were stained with a rabbit antibody directed against PLD2, PLD2-27 (A). These cells were costained with a mouse mAb to the *cis*-Golgi marker GM130 (B). (C) Overlapping regions between PLD2 and GM130. (D) Cells were stained with PLD2-27 antibody preincubated with 15 μg of PLD1 peptides before immunolocalization. (E) Preincubation of the PLD2-27 antibody with 1 μg of antigenic peptides before immunolocalization. (F) Corresponding phase contrast image of E. (G) Rat anterior pituitary GH_3 cells were stained with PLD2-27 antibody. Arrows highlight nuclear staining. (H) Preincubation of the PLD2-27 antibody with 1 μg of antigenic peptides before immunolocalization in GH_3 cells. (I) Corresponding phase contrast image of H. Images are from projected Z-series. Bars, 10 μm.

PLD2 localization in response to these drug treatments (Figure 5). In BFA-treated NRK cells, mannosidase II had a diffuse localization consistent with its redistribution to the ER (Figure 5B). Interestingly, BFA had little effect on the PLD2-positive puncta distributed in the cytoplasm, although as expected its Golgi-like staining was completely lost. Most significantly, after BFA treatment there was a striking enhancement of nuclear PLD2 staining (Figure 5A).

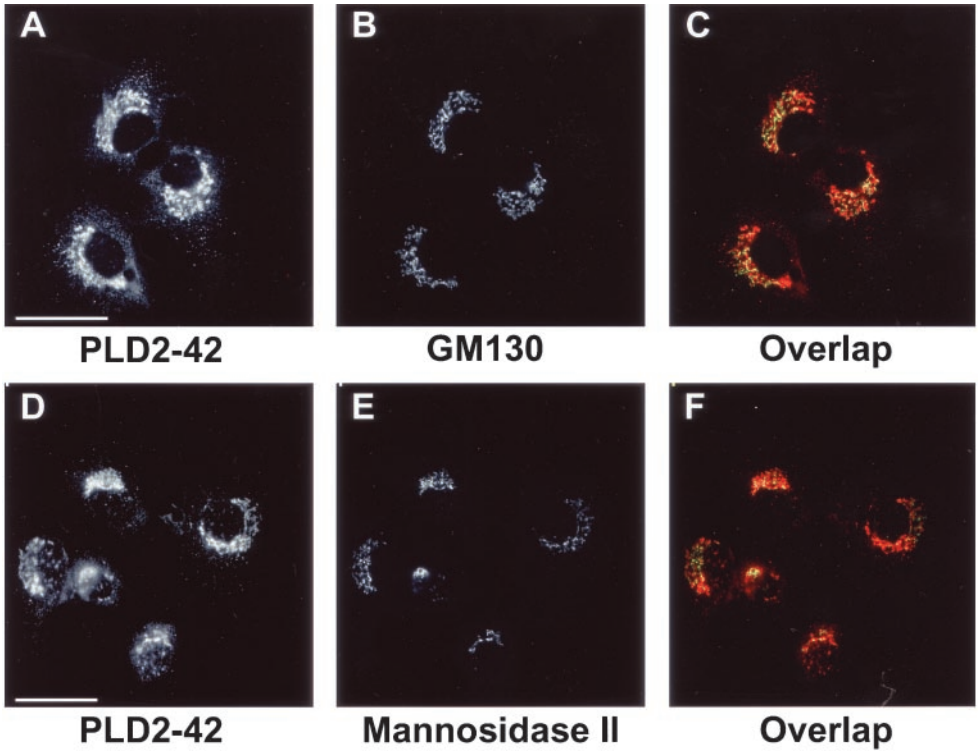

Figure 3. Immunolocalization of PLD2 by using an antibody generated to a different domain of the enzyme. (A and D) NRK cells were stained with PLD2-42, a rabbit polyclonal antibody directed against a peptide in the N terminus of PLD2 (see MATERIALS AND METHODS). The same fields of cells were costained with either a mouse mAb to GM130 (B) or with mAb 53FC3 to mannosidase II (E). Images were merged to determine overlap between PLD2-42 (red) and the respective Golgi markers (green). Areas of maximal overlap are yellow (C and F). Images are from projected Z-series. Bars, 10 μm.

This effect was identical to the translocation of PLD1 into the nucleus in both secretory and nonsecretory cells after BFA treatment (Freyberg *et al.*, 2001). Nuclear redistribution was very rapid; within 5 min of BFA treatment, PLD2 had lost its perinuclear localization and translocated to the nucleus (our unpublished data). Although possible, BFA may have induced redistribution of PLD2 to nuclear membranes rather than the nucleoplasm; however, this was unlikely given its staining pattern. Proteins, such as nuclear lamins, which localize to the nuclear envelope, show a ring-like staining pattern around the nucleus. PLD2, instead, was distributed throughout the nucleoplasm with distinct nucleolar exclusion, suggestive of a nuclear localization. Our observations that both PLD1 and PLD2 translocate to the nucleus after BFA treatment suggest that these enzymes play an as yet unspecified role(s) in nuclear signaling in response to the drug.

Nocodazole treatment of NRK cells led to redistribution of mannosidase II into large, peripheral Golgi membrane fragments (Figure 5E). However, unlike the response to BFA treatment, PLD2 retained its colocalization with mannosidase II–containing Golgi fragments with no significant nuclear translocation (Figure 5, D–F). Similar to BFA treatment, nocodazole did not disrupt the punctate cytoplasmic staining pattern of PLD2. This close association between PLD2 and Golgi fragments was identical to that of PLD1 and further suggests that PLD2 associates with Golgi membranes.

PLD2 Localizes to Golgi Rims

To define the localization of PLD2 in the Golgi apparatus more precisely, we used immunogold labeling of ultrathin cryosections incubated with affinity-purified PLD2 antibodies in GH_3 cells that have an extensive Golgi apparatus (Freyberg *et al.*, 2001) (Figures 6A and 7A). Gold particles were observed on multiple saccules of the Golgi apparatus, indicating that PLD2 was not limited to any one particular cisterna. Strikingly, virtually all PLD2 on the Golgi apparatus (94.1%; Table 1B) was localized to either cisternal rims or peri-Golgi vesicles. This contrasts dramatically with PLD1 (Figure 7B), which is localized throughout the Golgi cisternae, with only 25.3% that is associated with rims; the remainder being evenly distributed throughout the Golgi saccules (Freyberg *et al.*, 2001). Strikingly, quantitative analysis of PLD2 distribution demonstrated that it was enriched 80-fold in Golgi rims compared with cisternae, a finding that contrasts dramatically with that of PLD1, which showed little or no enrichment in rims (Table 1C). These data not only confirmed our immunofluorescence microscopy results but also demonstrated that PLD2 was unexpectedly confined to the rims of individual Golgi cisternae.

We coupled these observations with a stereological quantitation of total membrane volume for organelles (Griffiths *et al.*, 1989; Griffiths, 1993) to determine the extent of PLD2 enrichment in the Golgi apparatus (Table 2A). Although the percentage of PLD2-positive gold particles localized to Golgi apparatus, nucleus, and cytoplasm were similar (Table 1A), the volumes occupied by the respective organelles differed significantly (Table 2A). Consequently, PLD2 was enriched 25- and 21-fold in the Golgi apparatus compared with the nucleus and cytoplasm, respectively. Likewise, PLD1 was also highly enriched in the Golgi apparatus relative to the nucleus and cytoplasm (23- and 40-fold, respectively). A similarly significant enrichment of PLD2-immunoreactive

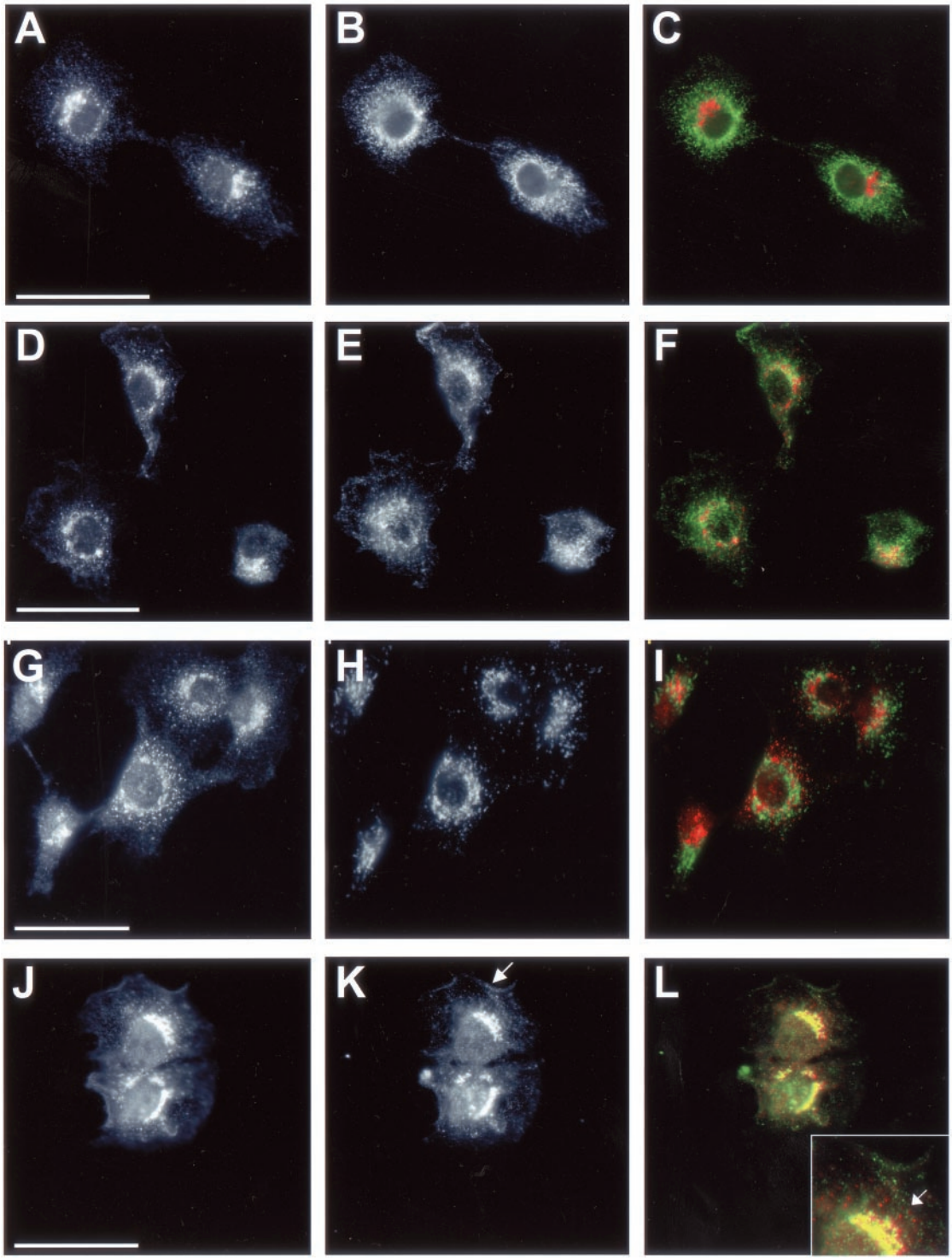

Figure 4. PLD2 localization with different organelles in rat NRK cells. Cells were prepared for immunofluorescence microscopy and incubated with rabbit PLD2 antibody PLD2-27 (A, D, G, and J) and costained with monoclonal antibodies to the ER marker BiP (B); the transferrin receptor (E), a marker of early endosomes and the plasma membrane; and lgp120 (H), a late endosome/lysosomal marker. (K) Cells were stained with caveolin-1, a marker for caveoli; the arrow corresponds to caveolin-1 localized to the plasma membrane. Images were merged to determine overlap between PLD2 (red) and the respective marker proteins (green; C, F, I, and L). Areas of maximal overlap are yellow. (L) Inset, enlargement of the region of overlap between PLD2 and caveolin-1 in the perinuclear Golgi apparatus. The arrow indicates areas where PLD2 puncta (red) either overlap completely with caveolin-1 (green) or are directly adjacent. Images are from projected Z-series. Bars, 10 μm.

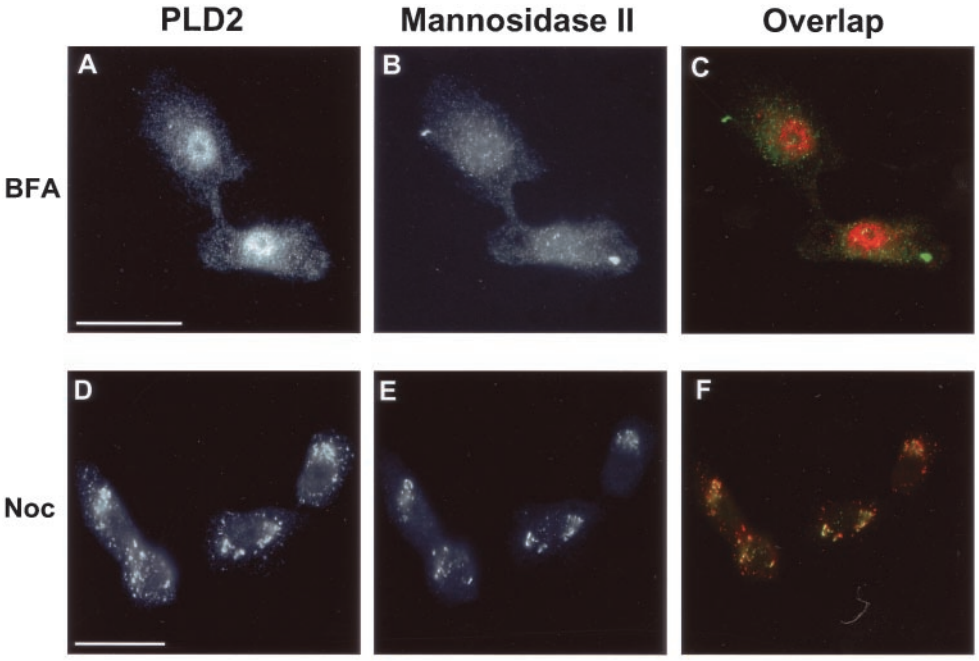

Figure 5. Brefeldin A and nocodazole alter the localization Golgi-associated PLD2. NRK cells were incubated with 5 μg BFA/ml for 40 min (A–C) or with 10 μM nocodazole for 4 h at 37°C (D–F). After incubation, cells were prepared for immunofluorescence microscopy by using the rabbit PLD2 antibody, PLD2-27 (A and D) or the 53FC3 mAb against mannosidase II (B and E). (A) Note the enrichment of PLD2 immunostaining in the cell nuclei. Bars, 10 μm.

gold particles in the Golgi apparatus relative to mitochondria (20-fold) and the endoplasmic reticulum (11.5-fold) was also observed (Table 2A). In addition, PLD2 was also present on the plasma membrane with a fraction localized to plasma membrane extensions (Figure 6B and Table 1B). Determination of the plasma membrane surface area relative to the Golgi apparatus (Table 2B) demonstrated an approximately threefold enrichment of PLD2 and a 4.5-fold enrichment of PLD1 in the Golgi apparatus relative to the plasma membrane. Furthermore, PLD2 was also localized to caveolae (Figure 6C), confirming our immunofluorescence microscopy observations as well as those of other investigators (Czarny *et al.*, 1999, 2000). Caveolae were defined according to their definition as uncoated flask-shaped vesicles continuous with the plasma membrane ranging from 50–100 nm in diameter (Razani *et al.*, 2002), and the absence of a visible

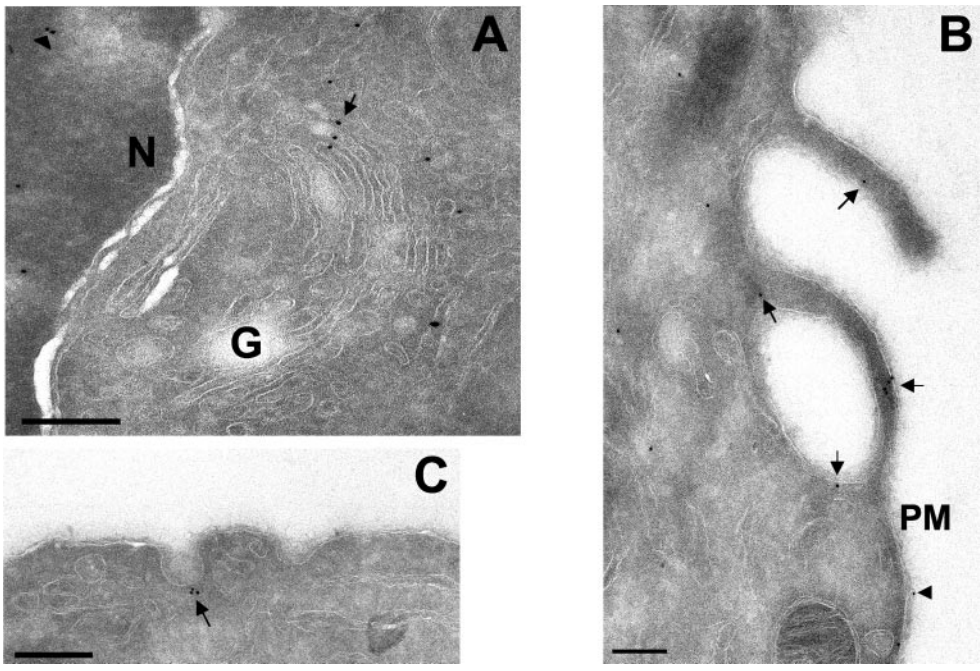

Figure 6. Localization of PLD2 by cryoimmunoelectron microscopy. Rat GH_3 cells were prepared for cryoimmunoelectron microscopy (see MATERIALS AND METHODS). Sections were labeled with affinity-purified rabbit polyclonal PLD2-27 antibodies followed by secondary antibodies conjugated to 10-nm gold particles. (A) PLD2 localized to the Golgi apparatus (G), particularly cisternal rims and peri-Golgi vesicles indicated by an arrow and to nuclei (N, arrowhead). (B) Plasma membrane localization of PLD2; arrows indicate areas of PLD2 staining. (C) Localization of PLD2 to caveolae (arrow). Bars, 0.2 μm.

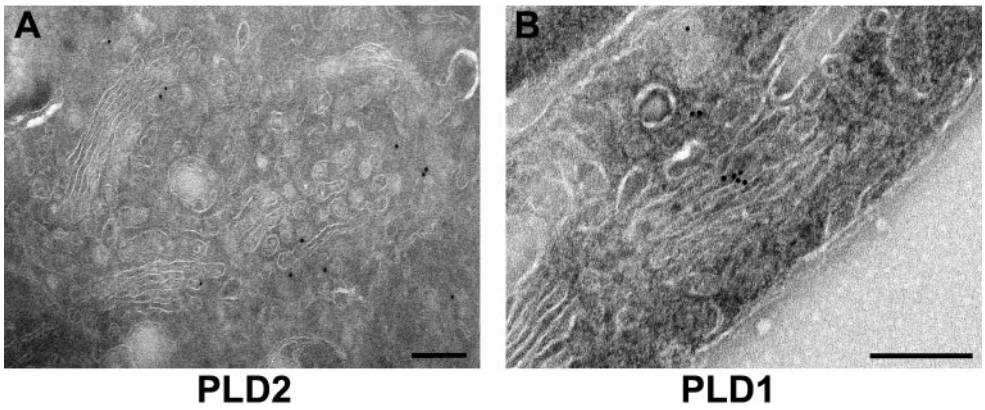

Figure 7. Comparison of PLD1 and PLD2 distribution in the Golgi apparatus: analysis by cryoimmunoelectron microscopy. Rat GH_3 cells were prepared for cryoimmunoelectron microscopy (see MATERIALS AND METHODS) and sections labeled with affinity-purified rabbit PLD2-27 antibody (A) or rabbit PLD1 (P1-P4) antibody (B) followed by secondary antibodies conjugated to 10-nm gold particles. Note the almost exclusive localization of PLD2 to Golgi rims and peri-Golgi vesicles, which contrasts with the cisternal staining of PLD1 antibodies. Bars, 0.2 μm.

coat made it unlikely that these invaginations were clathrin-coated pits. PLD2 gold labeling was evident on caveolae in various stages of invagination from the plasma membrane as well as adjacent to the characteristic omega-figures. Additionally, PLD2 was present on 100- to 200-nm intracellular vesicles as well as throughout the cytoplasm and the nucleus. Immunogold localization was specific because 1 μg of PLD2-specific peptides was sufficient to abolish all gold labeling (our unpublished data). Most significantly, these qualitative and quantitative results demonstrated that, relative to other organelles, PLD2 is distributed on the Golgi apparatus and is highly enriched (~80-fold) in the rims of the organelle.

DISCUSSION

Two principal isoforms of PLD have been documented in mammalian cells: PLD1 and PLD2 (Sung *et al.*, 1999; Liscovitch *et al.*, 2000). Both enzymes vary in their levels of activity; PLD1 has virtually no basal activity relative to PLD2 unless activated by protein kinase C or the small GTPases ARF1 or RhoA. In contrast, PLD2 has a robust level of constitutive activity (Liscovitch *et al.*, 2000). In addition, differences in localization between PLD1 and PLD2 have been documented (Liscovitch *et al.*, 2000); however, several of these studies have relied on overexpression of epitope- or fluorescently tagged PLD1 (Brown *et al.*, 1998; Toda *et al.*, 1999). Surprisingly, overexpressed PLD1 was absent from the Golgi apparatus and was localized to various intracellular compartments, including endosomes, lysosomes, secretory granules, and the plasma membrane (Brown *et al.*, 1998; Toda *et al.*, 1999). In contrast to these results, other laboratories, including our own, demonstrated ARF1-stimulated PLD1 activity on Golgi membranes (Ktistakis *et al.*, 1995; Chen *et al.*, 1997) and by using immunofluorescence and immunogold electron microscopy, localized the endogenous enzyme to the Golgi apparatus and nuclei in both secretory and nonsecretory cells (Freyberg *et al.*, 2001). These findings suggested that caution may be necessary when interpreting data from experiments that use overexpression protocols to define the subcellular localization of enzymes normally present only in catalytic amounts.

Recent work from our laboratory has demonstrated the importance of PA in maintaining the structure of the Golgi apparatus (Siddhanta *et al.*, 2000; Sweeney *et al.*, 2002). Given that PLD1 activity is low in the absence of activated ARF1, we speculated that Golgi structure may be maintained by a second source of PA, i.e., PLD2, and predicted that endogenous PLD2 was, at least partially, localized to the Golgi apparatus in addition to PLD1. To address this idea, we used highly specific antibodies directed against several PLD2 epitopes, and indirect immunofluorescence as well as cryoimmunogold electron microscopy. Herein, we have demonstrated that endogenous PLD2 has a widespread intracellular distribution with perinuclear enrichment and a punctate cytoplasmic staining pattern. This distribution differed markedly from previous studies by using PLD2 overexpression that localized the enzyme largely to the plasma membrane in resting REF-52 fibroblasts or with plasma membrane-localized EGF-receptor in human embryonic kidney 293 cells (Colley *et al.*, 1997; Slaaby *et al.*, 1998). On stimulation with serum, PLD2 becomes localized to submembranous structures indicative of endocytic vesicles (Colley *et al.*, 1997). Although we observed PLD2 localized to the plasma membrane, it was limited to discrete areas coincident with regions of membrane activity such as ruffles (Freyberg and Shields, unpublished observation) or transferrin receptor recycling (Figure 4). A distinct fraction of PLD2 also colocalized with caveolin-1 (Figure 4). This result is in agreement with evidence demonstrating that, by subcellular fractionation, PLD2, unlike PLD1, was present in caveolin-1-enriched low-density fractions (Czarny *et al.*, 1999, 2000). Our previous subcellular fractionation with rat liver was consistent with these findings (Sweeney *et al.*, 2002). The presence of PLD2 in caveolin-rich membrane compartments further supports our evidence, pointing to a role for the enzyme in regulating membrane dynamics. PLD1 and PLD2, in response to isoform-specific effector molecules, may individually or in concert alter the local composition of the plasma membrane to facilitate generation of the flask-like membrane invaginations that lead to formation of caveolae.

Recent evidence has suggested a role for PLD and PtdIns(4,5)P_2 in the nucleus. Nuclear PLD activity has been implicated in a diverse array of processes, including mitogenesis, apoptosis, and cell differentiation (Baldassare *et al.*, 1997; Martelli *et al.*, 1999; Neri *et al.*, 2002). Our previous study demonstrated that BFA treatment of GH_3 and NRK cells results in an altered PLD1 distribution; the enzyme

loses its Golgi localization, redistributes to the ER and acquires significantly enhanced nuclear staining (Freyberg *et al.*, 2001). Similarly, upon BFA treatment, we observed a major increase in PLD2 nuclear staining (Figure 5), establishing the presence of both PLD isoforms in the nucleus in response to collapse of the Golgi apparatus. Given that appearance of significant nuclear staining occurs within 5 min, the rapid kinetics of such an observation suggest that existing PLD2 was redistributed to the nucleus as opposed to generation of de novo-synthesized enzyme. Under these conditions, the proximity of ER-localized PLD2 (and PLD1) with the nuclear envelope may permit the enzymes' translocation into the nucleus; given the size (933 amino acids) of PLD2 it is highly unlikely to diffuse into the nucleus. Additionally, the absence of a nuclear localization signal in either PLD1 or PLD2 makes the possibility of passive diffusion into the nucleus even less likely. Recent evidence has shown that in response to differentiation stimuli, there is an increase in PtdIns(4,5)P_2-stimulated PLD activity in human promyelocytic leukemia HL-60 cells (Neri *et al.*, 2002). Given the presence of the phosphoinositide lipid synthesis machinery, including the PtdIns 4-kinase and PtdIns(4)P 5-kinases in the nucleus, PLD2 may play a role in the regulation of nuclear PtdIns(4,5)P_2 synthesis in a manner analogous to that at the Golgi apparatus (Boronenkov *et al.*, 1998; Walch-Solimena and Novick, 1999). With the localization of PtdIns(4,5)P_2 and the phosphoinositide lipid kinases to nuclear speckles, it is also possible that PLD may be involved in PtdIns(4,5)P_2-mediated pre-mRNA processing (Boronenkov *et al.*, 1998). We are currently investigating the individual roles of both PLD isoforms in the nucleus.

Interestingly, the localization of PLD2-positive peripheral puncta in the cytoplasm exhibited little change in distribution in response to BFA treatment (Figure 5A). Recent evidence has demonstrated that rapidly cycling ER-Golgi intermediate compartment protein ERGIC53 and Golgi matrix proteins such as GM130 and GRASP65 have a similar punctate appearance, in this case corresponding to ER exit sites (Ward *et al.*, 2001). The resemblance between the localization and appearance of golgin and ERGIC53-positive puncta and those of BFA-resistant PLD2 suggest the possibility that a fraction of the enzyme may also be present in ER exit sites. In support of this idea there was approximately twofold more PLD2 than PLD1 in the ER relative to its Golgi localization (Table 2A). Given the ability of PLD to stimulate vesicle budding in the Golgi apparatus, a potential role for PLD2 in regulating budding from ER exit sites is a possibility subject to further future examination.

Our morphological data agree with previous cell fractionation experiments with rat liver, where relatively little PLD2 was present in plasma membrane-enriched fractions (Sweeney *et al.*, 2002). Instead, the perinuclear distribution of PLD2 overlapped with several Golgi markers consistent with its localization to the perinuclear Golgi apparatus (Figures 1 and 2). This was verified by using cryoimmunogold electron microscopy and stereology that demonstrated the presence of PLD2 on the Golgi apparatus and other organelles (Figures 6 and 7; Tables 1 and 2). Unexpectedly, PLD2 was dramatically enriched (~80-fold) in the rims of the Golgi apparatus relative to cisternae (Table 1C) and its level was approximately threefold higher in Golgi membranes compared with the plasma membrane (Table 2). This distribution is in marked contrast to that of PLD1, which is present throughout Golgi cisternae and enriched only approximately twofold in the cisternal rims (Figure 7B and Table 1C; Freyberg *et al.*, 2001). The differential distribution of PLD1 and PLD2 may indicate that these enzymes have separate functions in the Golgi apparatus. In light of these differences, we speculate that PLD2 may function as a "housekeeping" enzyme, whereas ARF1-activated PLD1 plays a role in regulating PA in response to stimuli. Such a model would be consistent with the relatively high basal activity of PLD2 compared with PLD1. The constitutive basal PLD2 activity may serve to generate and maintain a steady-state pool of PA, and indirectly the PtdIns(4,5)P_2 necessary for the structural integrity of the Golgi apparatus (Siddhanta *et al.*, 2000; Sweeney *et al.*, 2002). It is also possible that the rim localization of PLD2 implies a regulatory role in mediating vesicular trafficking analogous to the recent observations that protein components of the retrograde transport machinery are localized to rims of the Golgi apparatus (Martinez-Menarguez *et al.*, 2001; Luna *et al.*, 2002). The localization of Cdc42 and PLD2 to Golgi rims and their respective interactions with the actin cytoskeleton are consistent with such a model (Colley *et al.*, 1997; Luna *et al.*, 2002). Furthermore, in catalyzing the hydrolysis of phosphatidylcholine to PA, PLD2 may alter the local membrane composition at the cisternal rims to facilitate release of vesicles. Consistent with this idea, endophilin, a protein implicated in synaptic vesicle endocytosis, also generates PA, although from a different precursor, lysophosphatidic acid. It has been suggested that increasing local concentrations of PA, as mediated by endophilin, alter membrane curvature sufficiently to facilitate vesicular budding (Schmidt *et al.*, 1999). Taken together, our evidence suggests a distinct role for PLD2 in regulating the membrane composition of Golgi rims. The roles of PLD1 and PLD2 in regulating the organization of the Golgi apparatus are currently under investigation.

ACKNOWLEDGMENTS

This work was supported by National Institutes of Health grant DK-21860 to D.S. Core support was provided by National Institutes of Health Cancer Center grant P30CA13330. We thank Michael Cammer for help with immunofluorescence microscopy and especially Frank Macaluso, Leslie Gunther-Cummins, and Carolyn Marks for superb expert technical assistance with electron microscopy; Dr. Brian Burke for generous gifts of antibodies as well as Dr. Anirban Siddhanta, Dr. Som Ming Leung, Raymond Chiu, and Leonid Novikov for helpful discussions and suggestions with the manuscript.

REFERENCES

Austin, C.D., and Shields, D. (1996). Formation of nascent secretory vesicles from the trans-Golgi network of endocrine cells is inhibited by tyrosine kinase and phosphatase inhibitors. J. Cell Biol. *135*, 1471–1483.

Baldassare, J.J., Jarpe, M.B., Alfres, L., and Raben, D.M. (1997). Nuclear translocation of RhoA mediates the mitogen-induced activation of phospholipase D involved in nuclear envelope signal transduction. J. Biol. Chem. *272*, 4911–4914.

Baldassare, J.J., Klaus, J., Phillips, P.J., and Raben, D.M. (2001). PLD1b in IIC9 fibroblasts is selectively activated in the nucleus and not in the Golgi apparatus. Cell Biol. Int. *25*, 1207–1212.

Boronenkov, IV, Loijens, J.C., Umeda, M., and Anderson, R.A. (1998). Phosphoinositide signaling pathways in nuclei are associated with nuclear speckles containing pre-mRNA processing factors. Mol. Biol. Cell *9*, 3547–3560.

Brown, F.D., Thompson, N., Saqib, K.M., Clark, J.M., Powner, D., Thompson, N.T., Solari, R., and Wakelam, M.J. (1998). Phospholipase D1 localizes to secretory granules and lysosomes and is plasma-membrane translocated on cellular stimulation. Curr. Biol. *8*, 835–838.

Brown, H.A., Gutowski, S., Moomaw, C.R., Slaughter, C., and Sternweis, P.C. (1993). ADP-ribosylation factor, a small GTP-dependent regulatory protein, stimulates phospholipase D activity. Cell *75*, 1137–1144.

Chen, Y.G., Siddhanta, A., Austin, C.D., Hammond, S.M., Sung, T.C., Frohman, M.A., Morris, A.J., and Shields, D. (1997). Phospholipase D stimulates release of nascent secretory vesicles from the trans-Golgi network. J. Cell Biol. *138*, 495–504.

Colley, W.C., Sung, T.C., Roll, R., Jenco, J., Hammond, S.M., Altshuller, Y., Bar-Sagi, D., Morris, A.J., and Frohman, M.A. (1997). Phospholipase D2, a distinct phospholipase D isoform with novel regulatory properties that provokes cytoskeletal reorganization. Curr. Biol. *7*, 191–201.

Cremona, O., and De Camilli, P. (2001). Phosphoinositides in membrane traffic at the synapse. J. Cell Sci. *114*, 1041–1052.

Czarny, M., Fiucci, G., Lavie, Y., Banno, Y., Nozawa, Y., and Liscovitch, M. (2000). Phospholipase D2: functional interaction with caveolin in low-density membrane microdomains. FEBS Lett. *467*, 326–332.

Czarny, M., Lavie, Y., Fiucci, G., and Liscovitch, M. (1999). Localization of phospholipase D in detergent-insoluble, caveolin-rich membrane domains. Modulation by caveolin-1 expression and caveolin-1. J. Biol. Chem. *274*, 2717–2724.

De Camilli, P., Emr, S.D., McPherson, P.S., and Novick, P. (1996). Phosphoinositides as regulators in membrane traffic. Science *271*, 1533–1539.

Freyberg, Z., Sweeney, D., Siddhanta, A., Bourgoin, S., Frohman, M., and Shields, D. (2001). Intracellular localization of phospholipase D1 in mammalian cells. Mol. Biol. Cell *12*, 943–955.

Ganley, IG., Walker, S.J., Manifava, M., Li, D., Brown, H.A., and Ktistakis, N.T. (2001). Interaction of phospholipase D1 with a casein-kinase-2-like serine kinase. Biochem. J. *354*, 369–378.

Griffiths, G. (1993). Fine Structure Immuno-cytochemistry, Berlin: Springer Verlag.

Griffiths, G., Fuller, S.D., Back, R., Hollinshead, M., Pfeiffer, S., and Simons, K. (1989). The dynamic nature of the Golgi complex. J. Cell Biol. *108*, 277–297.

Hammond, S.M., Jenco, J.M., Nakashima, S., Cadwallader, K., Gu, Q., Cook, S., Nozawa, Y., Prestwich, G.D., Frohman, M.A., and Morris, A.J. (1997). Characterization of two alternately spliced forms of phospholipase D1. Activation of the purified enzymes by phosphatidylinositol 4,5-bisphosphate, ADP-ribosylation factor, and Rho family monomeric GTP-binding proteins and protein kinase C-α. J. Biol. Chem. *272*, 3860–3868.

Honda A., Nogami M., Yokozeki M., Nakamura H., Watanabe H., Kawamoto K., Nakaya K., Morris AJ, Frohman MA, and Kanaho Y. (1999). Phosphatidylinositol 4-phosphate 5-kinase alpha is a downstream effector of the small G protein ARF6 in membrane ruffle formation. Cell *99*, 521–532.

Houle, M.G., and Bourgoin, S. (1999). Regulation of phospholipase D by phosphorylation-dependent mechanisms. Biochim. Biophys. Acta *1439*, 135–149.

Humeau, Y., Vitale, N., Chasserot-Golaz, S., Dupont, J.L., Du, G., Frohman, M.A., Bader, M.F., and Poulain, B. (2001). A role for phospholipase D1 in neurotransmitter release. Proc. Natl. Acad. Sci. USA *98*, 15300–15305.

Jenkins, G.H., Fisette, P.L., and Anderson, R.A. (1994). Type I phosphatidylinositol 4-phosphate 5-kinase isoforms are specifically stimulated by phosphatidic acid. J. Biol. Chem. *269*, 11547–11554.

Joseph, T., Wooden, R., Bryant, A., Zhong, M., Lu, Z., and Foster, D.A. (2001). Transformation of cells overexpressing a tyrosine kinase by phospholipase D1 and D2. Biochem. Biophys. Res. Commun. *289*, 1019–1024.

Kam, Y., and Exton, J.H. (2001). Phospholipase D activity is required for actin stress fiber formation in fibroblasts. Mol. Cell. Biol. *21*, 4055–4066.

Kim, Y., Kim, J.E., Lee, S.D., Lee, T.G., Kim, J.H., Park, J.B., Han, J.M., Jang, S.K., Suh, P.G., and Ryu, S.H. (1999). Phospholipase D1 is located and activated by protein kinase C alpha in the plasma membrane in 3Y1 fibroblast cell. Biochim. Biophys. Acta *1436*, 319–330.

Ktistakis, N.T., Brown, H.A., Sternweis, P.C., and Roth, M.G. (1995). Phospholipase D is present on Golgi-enriched membranes and its activation by ADP ribosylation factor is sensitive to brefeldin A. Proc. Natl. Acad. Sci. USA *92*, 4952–4956.

Ktistakis, N.T., Brown, H.A., Waters, M.G., Sternweis, P.C., and Roth, M.G. (1996). Evidence that phospholipase D mediates ADP ribosylation factor-dependent formation of Golgi coated vesicles. J. Cell Biol. *134*, 295–306.

Lippincott-Schwartz, J., Yuan, L.C., Bonafacino, J.S., and Klausner, R.D. (1989). Rapid redistribution of Golgi proteins into the ER in cells treated with brefeldin A: evidence for membrane cycling from Golgi to ER. Cell *56*, 801–813.

Liscovitch, M., Czarny, M., Fiucci, G., and Tang, X. (2000). Phospholipase D: molecular and cell biology of a novel gene family. Biochem. J. *345*, 401–415.

Lopez, I, Arnold, R.S., and Lambeth, J.D. (1998). Cloning and initial characterization of a human phospholipase D2 (hPLD2). ADP-ribosylation factor regulates hPLD2. J. Biol. Chem. *273*, 12846–12852.

Lowe, M., Gonatas, N.K., and Warren, G. (2000). The mitotic phosphorylation cycle of the *cis*-Golgi matrix protein GM130. J. Cell Biol. *149*, 341–356.

Luna, A., Matas, O.B., Martínez-Menárguez, J.A., Mato, E., Durán, J.M., Ballesta, J., Way, M., and Egea, G. (2002). Regulation of Protein Transport from the Golgi Complex to the Endoplasmic Reticulum by CDC42 and N-WASP. Mol. Biol. Cell *13*, 866–879.

Marcil, J., Harbor, D., Naccache, P.H., and Bourgoin, S. (1997). Human phospholipase D1 can be tyrosine-phosphorylated in HL-60 granulocytes. J. Biol. Chem. *272*, 20660–20664.

Martelli, A.M., Bortul, R., Bareggi, R., Tabellini, G., Grill, V, Baldini, G., and Narducci, P. (1999). The pro-apoptotic drug camptothecin stimulates phospholipase D activity and diacylglycerol production in the nucleus of HL-60 human promyelocytic leukemia cells. Cancer Res. *59*, 3961–3967.

Martin, T.F. (2001). PI(4,5)P_2 regulation of surface membrane traffic. Curr. Opin. Cell Biol. *13*, 493–499.

Martinez-Menarguez, J.A., Prekeris, R., Oorschot, V.M., Scheller, R., Slot, J.W., Geuze, H.J., and Klumperman, J. (2001). Peri-Golgi vesicles contain retrograde but not anterograde proteins consistent with the cisternal progression model of intra-Golgi transport. J. Cell Biol. *155*, 1213–1224.

Neri, L.M., Bortul, R., Borgatti, P., Tabellini, G., Baldini, G., Capitani, S., and Martelli, A.M. (2002). Proliferating or differentiating stimuli

act on different lipid-dependent signaling pathways in nuclei of human leukemia cells. Mol. Biol. Cell *13*, 947–964.

Razani, B., Combs, T.P., Wang, X.B., Frank, P.G., Park, D.S., Russell, R.G., Li, M., Tang, B., Jelicks, L.A., Scherer, P.E., and Lisanti, M.P. (2002). Caveolin-1-deficient mice are lean, resistant to diet-induced obesity, and show hyper-triglyceridemia with adipocyte abnormalities. J. Biol. Chem. *277*, 8635–8647.

Sarkar, S., Miwa, N., Kominami, H., Igarashi, N., Hayashi, S., Okada, T., Jahangeer, S., and Nakamura, S. (2001). Regulation of mammalian phospholipase D2: interaction with and stimulation by G(M2) activator. Biochem. J. *359*, 599–604.

Schmidt, A., Wolde, M., Thiele, C., Fest, W., Kratzin, H., Podtelejnikov, A.V, Witke, W., Huttner, W.B., and Soling, H.D. (1999). Endophilin I mediates synaptic vesicle formation by transfer of arachidonate to lysophosphatidic acid. Nature *401*, 133–141.

Shen, Y., Xu, L., and Foster, D.A. (2001). Role for phospholipase D in receptor-mediated endocytosis. Mol. Cell. Biol. *21*, 595–602.

Siddhanta, A., Backer, J.M., and Shields, D. (2000). Inhibition of phosphatidic acid synthesis alters the structure of the Golgi apparatus and inhibits secretion in endocrine cells. J. Biol. Chem. *275*, 12023–12031.

Slaaby, R., Jensen, T., Hansen, H.S., Frohman, M.A., and Seedorf, K. (1998). PLD2 complexes with the EGF receptor and undergoes tyrosine phosphorylation at a single site upon agonist stimulation. J. Biol. Chem. *273*, 33722–33727.

Sung, T.C., Altshuller, Y.M., Morris, A.J., and Frohman, M.A. (1999). Molecular analysis of mammalian phospholipase D2. J. Biol. Chem. *274*, 494–502.

Sweeney, D.A., Siddhanta, A., and Shields, D. (2002). Fragmentation and re-assembly of the Golgi apparatus in vitro. A requirement for phosphatidic acid and phosphatidylinositol 4,5-bisphosphate synthesis. J. Biol. Chem. *277*, 3030–3039.

Toda, K., Nogami, M., Murakami, K., Kanaho, Y., and Nakayama, K. (1999). Colocalization of phospholipase D1 and GTP-binding-defective mutant of ADP-ribosylation factor 6 to endosomes and lysosomes. FEBS Lett. *442*, 221–225.

Walch-Solimena, C., and Novick, P. (1999). The yeast phosphatidylinositol-4-OH kinase pik1 regulates secretion at the Golgi. Nat. Cell Biol. *1*, 523–525.

Ward, T.H., Polishchuk, R.S., Caplan, S., Hirschberg, K., and Lippincott-Schwartz, J. (2001). Maintenance of Golgi structure and function depends on the integrity of ER export. J. Cell Biol. *155*, 557–570. .0